Proceedings of 8th International Conference on Mechanical Engineering and Renewable Energy 2025
10-12 December, 2025, Chattogram, BANGLADESH
SciEn Conference Series: Engineering Vol. 4, 2026, pp 78-86 https://doi.org/10.38032/scse.2026.4.43

Design and Fabrication of One Shell Pass and Two Tube Pass Heat Exchanger

Golam Saklayen, Bodius Salam, Md. Fardim Hasan Emon, and Md. Mamunur Rahman*

Department of Mechanical Engineering, Chittagong University of Engineering & Technology, Chattogram-4349, Bangladesh

ABSTRACT

High-efficiency heat exchangers are essential to meet the growing industrial demand for maximizing thermal energy transfer. Shell-and-tube heat exchangers (STHEs) serve as standard components in heating, ventilation, and air conditioning (HVAC) systems due to their large heat transfer surface area, making them particularly suitable for chiller operations. This research presents the complete design, fabrication, and performance evaluation of an STHE configured with one shell pass and two tube passes. The study analyzes how system performance is affected by different hot and cold fluid mass flow rates while maintaining the inlet temperatures constant. Using a laboratory-scale, experimental analysis produced effectiveness (ε) values between 0.096 and 0.173 and log mean temperature difference (LMTD) values between 26.99 °C and 28.57 °C. Precise measurements and calculations provided critical insights into key thermal performance parameters. These includes heat transfer rates, overall heat transfer coefficients, and convective heat transfer coefficients The findings contribute to understanding of multipass STHE behavior and provide direction for the design of more effective thermal energy systems for operations.

Keywords: Heat Exchanger, LMTD, Heat Transfer, Efficiency, Fabrication

1. Introduction

Heat exchangers are essential thermal systems designed to transfer energy efficiently between two or more fluids at different temperatures while maintaining physical separation. This transfer occurs primarily through conduction, convection, and, in some cases, radiation [1]. They play a vital role in improving energy efficiency and temperature control across numerous industries. These are HVAC, power generation, refrigeration, chemical processing, and petrochemicals, where they help minimize energy losses and optimize overall system performance [2]. Among the various configurations, shell-and-tube heat exchangers (STHEs) are the most commonly used due to their mechanical strength, scalability, and capability to operate under high pressure and temperature conditions [3]. They are widely applied in processes such as oil and condensate cooling, boiler feedwater preheating, cooling tower operations, and industrial fluid heating or cooling [4]. However, conventional single-pass STHEs often exhibit lower thermal performance, mainly because of restricted flow distribution and limited heat transfer surface area [5]. To overcome these limitations, multi-pass designs, especially those with one shell pass and multiple tube passes, have gained significant attention. These configurations promote improved heat transfer by increasing fluid residence time and enhancing turbulence within the tubes, leading to better energy exchange without substantially increasing the manufacturing complexity [6].

Over the past few decades, a considerable amount of research has focused on the design, fabrication, and performance enhancement of STHEs. The motivation has largely centered on improving thermal efficiency, reducing operational costs, and addressing issues such as pressure drop and fouling. The classical studies by Yılmaz and Unverdi [7] remain foundational, introducing analytical approaches like the log mean temperature difference (LMTD) and the effectiveness, number of transfer units (ε-NTU) methods, both of which continue to guide exchanger sizing and performance evaluation. Building upon these fundamentals, Silaipillayarputhur and Mughanam [8] explored the impact of geometric features, particularly tube arrangement, baffle design, and material choice on the overall heat transfer capability of STHEs. In more recent years, attention has shifted toward computational and optimization-based design methods that balance energy performance with cost efficiency. Tahery et al. [9] developed multi-objective optimization models that integrated tube bundle geometry and economic parameters, achieving 10–24% reductions in annualized cost through genetic algorithms. Similarly, Tuncer et al. [4] improved the thermal performance of helical-coil exchangers by altering shell geometry and validating the outcomes through both simulation and experiment. The review by Hadad et al. [10] offered a broader perspective on emerging enhancement techniques, highlighting nanofluids as an effective way to boost convective heat transfer coefficients by up to 30% [11,12]. Multipass shell-and-tube designs have drawn significant interest for their compactness and higher effectiveness compared with traditional single-pass configurations. Ortega et al. [13] introduced optimization algorithms capable of handling uncertain operational parameters, showing that such models can maintain strong performanceunder varying flow and temperature conditions. Ahmad et al. [14] further refined multipass design theory by challenging a long-accepted rule and proposed a combined thermal–hydraulic modeling framework for more accurate design predictions. Experimentally, Guimaraes et al. [15] constructed a small-scale, two-tube-pass exchanger for

*Corresponding Author Email Address: fardim.emon@gmail.com

laboratory use and reported LMTD values between 25 °C and 30 °C, with effectiveness reaching 0.2 under steady flow conditions, demonstrating the promise of these configurations for educational and low-cost industrial systems. Research into fabrication methods and materials has also evolved. Marzouk et al. [16] developed a laboratory-scale STHE using stainless steel and rubber gaskets for improved sealing, noting that spatial constraints limited the number of tubes. High-conductivity materials such as copper and copper–nickel alloys have been adopted to achieve higher heat transfer rates, although their cost remains a limiting factor. In parallel, Qian et al. [17] examined helically baffled exchangers and achieved roughly 20% gains in efficiency due to enhanced turbulence and secondary flow formation. Nanofluid-based and geometrically modified exchangers have recently become another area of active investigation. Hussien et al. [18] reported that the use of nanofluids increased the Nusselt number by 20-40%, though challenges related to particle stability and fouling still persist. Studies by Boujelbene et al. [19] indicated that twisted and finned tube designs can raise heat transfer rates by 10-25%, providing practical solutions for systems operating under elevated pressures and temperatures. The introduction of corrosion-resistant alloys and additive manufacturing technologies has further been predicted to reduce industrial energy use by up to 15% by 2030 [20]. Despite these advances, some key issues remain unresolved. Laboratory scale multipass STHEs often face fabrication challenges tied to limited tube counts and material costs [21]. Moreover, the influence of Reynolds number variation on convective heat transfer in small, low-flow-rate exchangers is still not well documented [22].

While numerical modeling and CFD optimization dominate current studies, there is a noticeable gap in experimental datasets reflecting real operating conditions. The main objective of this research is to design and fabricate a one-shell pass and two-tube pass heat exchanger that can be used as a laboratory apparatus. Due to its intended use in a laboratory setting, the constructional materials chosen for this apparatus will be stainless steel. The number of tubes utilized will be limited to 10 due to spatial constraints. To increase the effectiveness and efficiency of the heat exchanger, copper can be employed instead of stainless steel. While water will be the primary working fluid, it can also be substituted with high convective fluids or nanofluids to achieve superior efficiency.

2. Methodology

Heat exchangers function as mechanisms that facilitate thermal energy transfer across fluids with varying temperatures.

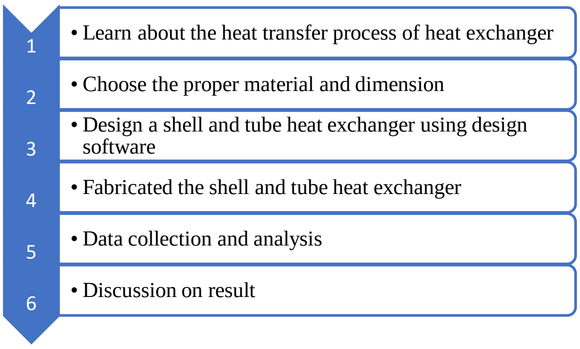

Fig. 1 Flow chart on project methodology

The primary objective in using this equipment within a laboratory environment is to gain an understanding of the manufacturing process, along with comprehending the heat transfer mechanism between the two fluids. To facilitate water circulation through the heat exchanger, a pump will be utilized. The sequential methodology (Fig. 1) for this particular case is explained in detail in the subsequent section of this section.

2.1 Proposed Model

The proposed model (Fig. 2) has been introduced due to its distinct advantages over traditional heat exchangers. Its intricate design complexity prevents it from being easily disassembled Fig. 3. This model is particularly valuable for handling fluids that are prone to contamination. The header dimensions are shown Fig. 4, while the tube spacing and tube dimensions are presented Fig. 5 and Fig. 6, respectively. In contrast to a single-pass shell and tube heat exchanger, the proposed model allows the fluid to travel twice, resulting in enhanced heat transfer due to the larger surface area. Furthermore, increasing the number of tubes can further augment heat transfer.

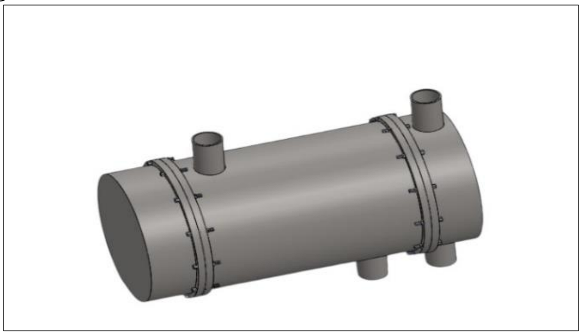

Fig. 2 One shell pass and two tube pass heat exchanger

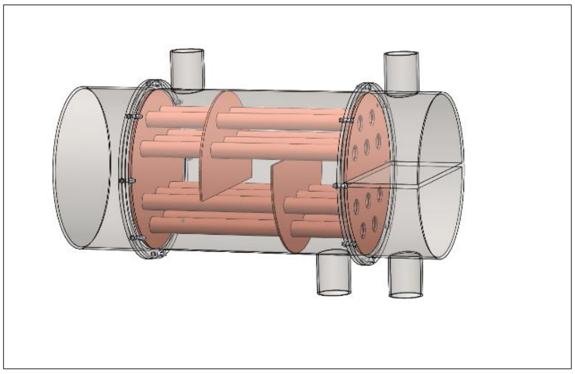

Fig. 3 Internal view of the heat exchanger

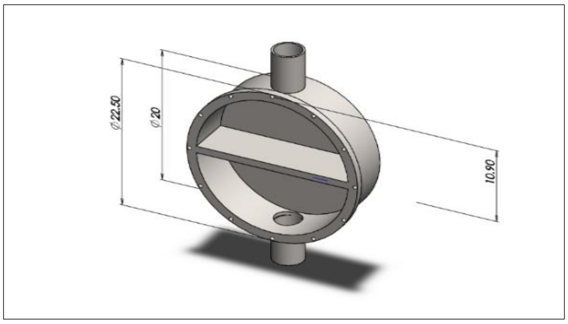

Fig. 4 Dimensions of header

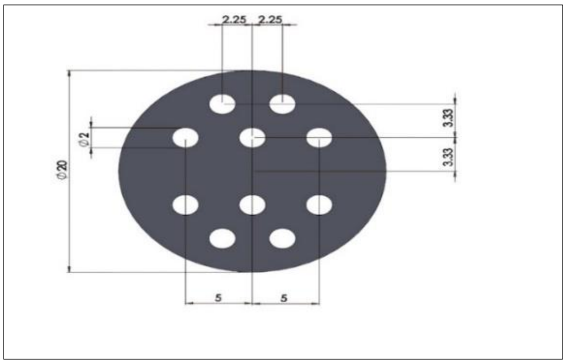

Fig. 5 Dimensions of tube spacing

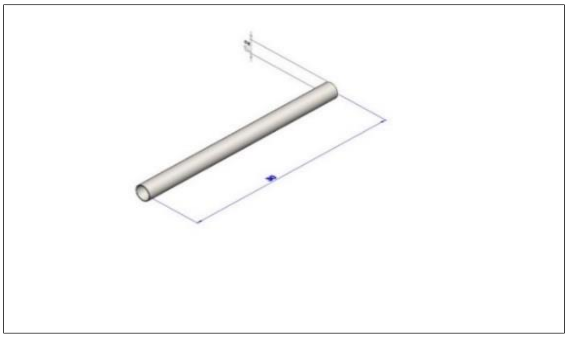

Fig. 6 Dimensions of tube

2.2 Fabrication and Experimental Setup

The heat exchanger components were fabricated with precision, adhering to the specified dimensions and shape, and utilizing stainless steel material. To ensure airtightness, rubber gaskets were incorporated into the design. The heat exchanger (Fig. 7) consisted of ten tubes, with five tubes positioned in the upper part of the shell and five in the lower part.

Fig. 7 Shell and tube heat exchanger

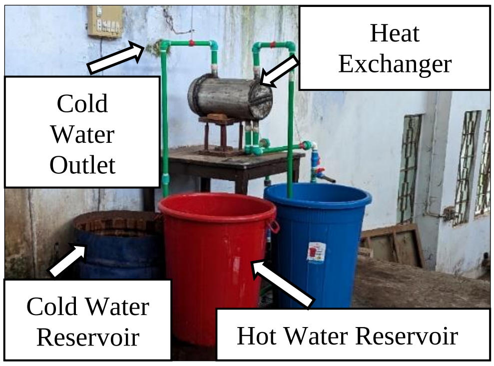

Fig. 8 Experimental setup

An experimental setup (Fig. 8) was constructed to measure the efficiency, log mean temperature difference, and overall heat transfer performance of the shell and tube heat exchanger. The assembled shell and tube heat exchanger (Fig. 9) used in the experiment.

Fig. 9 Shell and tube heat exchanger

3. Data Collection and Calculation

3.1 Data Collection

These table contains water temperatures and mass flow rates of the inlet and outlet when the hot water flow rate is gradually increased and the cold water flow rate remains constant at their respective LPM.

Table 1 contains mass flow rates and water temperatures of the inlet and outlet when the hot water flow rate is gradually increased.

Table 1 Data table for a constant hot water flow rate at 4 LPM

Data No.	Hot water (Inside tube)			
	m_h (LPM)	m_h (kg/s)	$T_{h,in}$ (^OC)	$T_{h,out}$ (^OC)
1	4	0.066	58	52
2	5	0.082	58	52.7
3	6	0.098	57.9	53.1
4	7	0.115	57.8	53.5
5	8	0.131	57.8	53.8

Table 2 contains mass flow rates and water temperatures of the inlet and outlet when the cold water flow rate remains constant at 4 LPM.

Table 2 Data table for a constant cold water flow rate at 4 LPM

Data No.	Cold water (Outside tube)			
	m_c (LPM)	m_c (kg/s)	$T_{c,in}$ (^OC)	$T_{c,out}$ (^OC)
1	4	0.067	26	30
2	4	0.067	26	30.7
3	4	0.067	26	31
4	4	0.067	26	31.3
5	4	0.067	26	31.5

Table 3 contains mass flow rates and water temperatures of the inlet and outlet when the hot water flow rate is gradually increased.

Table 3 Data table for a constant hot water flow rate at 8 LPM

Data No.	Hot water (Inside tube)			
	m_h (LPM)	m_h (kg/s)	$T_{h,in}$ (^OC)	$T_{h,out}$ (^OC)
1	4	0.066	58.2	51.8
2	5	0.082	58.1	52.4
3	6	0.098	58	52.9
4	7	0.115	58	53.4
5	8	0.131	57.8	53.6

Table 4 contains mass flow rates and water temperatures of the inlet and outlet when the cold water flow rate remains constant at 8 LPM.

Table 4 Data table for a constant cold water flow rate at 8 LPM

Data No.	Cold water (Outside tube)			
	m_c (LPM)	m_c (kg/s)	$T_{c,in}$ (^OC)	$T_{c,out}$ (^OC)
1	8	0.13	26	28.2
2	8	0.13	26	28.5
3	8	0.13	26	28.6
4	8	0.13	26	28.8
5	8	0.13	26	29

Table 5 contains mass flow rates and water temperatures of the inlet and outlet when the hot water flow rate is gradually increased.

Table 5 Data table for a constant hot water flow rate at 12 LPM

Data No.	Hot water (Inside tube)			
	m_h (LPM)	m_h (kg/s)	$T_{h,in}$ (^OC)	$T_{h,out}$ (^OC)
1	4	0.066	57.8	51.4
2	5	0.082	57.8	52
3	6	0.099	57.6	52.4
4	7	0.115	57.5	52.8
5	8	0.131	57.4	53

Table 6 contains mass flow rates and water temperatures of the inlet and outlet when the cold water flow rate remains constant at 12 LPM.

Table 6 Data table for a constant cold water flow rate at 12 LPM

Data No.	Cold water (Outside tube)			
	m_c (LPM)	m_c (kg/s)	$T_{c,in}$ (^OC)	$T_{c,out}$ (^OC)
1	12	0.2	26	27.5
2	12	0.2	26	27.7
3	12	0.2	26	27.8
4	12	0.2	26	27.9
5	12	0.2	26	28

Table 7 contains the mass flow rate and water temperatures of the inlet and outlet when the hot water flow rate is gradually increased.

Table 7 Data table for a constant hot water flow rate at 16 LPM

Data No.	Hot water (Inside tube)			
	m_h (LPM)	m_h (kg/s)	$T_{h,in}$ (^OC)	$T_{h,out}$ (^OC)
1	4	0.066	58.1	51.4
2	5	0.082	58	52.1
3	6	0.099	58	52.6
4	7	0.115	57.8	52.9
5	8	0.131	57.6	53.1

Table 8 contains mass flow rates and water temperatures of the inlet and outlet when the cold water flow rate remains constant at 16 LPM.

Table 8 Data table for a constant cold water flow rate at 16 LPM

Data No.	Cold water (Outside tube)			
	m_c (LPM)	m_c (kg/s)	$T_{c,in}$ (^OC)	$T_{c,out}$ (^OC)
1	16	0.266	26	27.2
2	16	0.266	26	27.3
3	16	0.266	26	27.4
4	16	0.266	26	27.5
5	16	0.266	26	27.7

4. Mathematical Equations

Required equations Eq. (1)-(9) for calculation are as follows:

Heat release by hot fluid,

$$Q_h = m_h \times C_p \times (T_{h,in} - T_{h,out}) \quad (1)$$

Heat received by cold fluid,

$$Q_c = m_c \times C_p \times (T_{c,out} - T_{c,in}) \quad (2)$$

Log mean temperature difference,

$$LMTD = \frac{(T_{h,in}-T_{c,out})-(T_{h,out}-T_{c,in})}{ln(\frac{T_{h,in}-T_{c,out}}{T_{h,out}-T_{c,in}})} \quad (3)$$

Effectiveness,

$$\mathcal{E} = \frac{m_c \times C_p \times (T_{c,out}-T_{c,in})}{(m \times C_p)_{min} \times (T_{h,in}-T_{c,in})} \quad (4)$$

Overall heat transfer coefficient,

$$U = \frac{Q_c}{F \times LMTD \times A} \quad (5)$$

Reynolds Number,

$$Re = \frac{\rho \times V \times D_i}{\mu} \quad (6)$$

Nusselt Number,

$$Nu = 3.66 + \frac{0.0668 \times (D_i/L) \times Re \times Pr}{1+0.04[(D_i/L) \times Re \times Pr]^{2/3}} \quad (7)$$

Heat transfer through a cylindrical tube surface,

$$Q = \frac{T_1-T_2}{\frac{1}{A_i \times h_i} + \frac{ln(\frac{r_o}{r_i})}{2 \times \pi \times k \times L} + \frac{1}{A_o \times h_o}} \quad (8)$$

Convective heat transfer coefficient outside tube,

$$h_o = [(A_o) \times (\frac{T_1-T_2}{Q} - \frac{1}{h_i \times A_i} - \frac{ln(\frac{r_o}{r_i})}{2 \times \pi \times k \times L})]^{-1} \quad (9)$$

Table 9 includes the calculated values obtained as the hot water flow rate increases gradually.

Table 9 Tabulated data presenting calculated values for Case 1 (4 LPM)

Data No.	Q_h (W)	Q_c (W)	LMTD (^OC)	U (W/m^2.k)
1	1655.28	1120.24	26.99	173.96
2	1818.59	1309.74	27	207.13
3	1976.24	1393.33	27	220.27
4	2065.29	1476.93	27	233.4
5	2195.66	1532.67	27.04	241.74

Table 10 includes the calculated values obtained as the hot water flow while the cold water flow rate is held constant at 4 LPM.

Table 10 Tabulated data presenting calculated values for Case 1 (4 LPM)

Data No.	Re	$\mathcal{E}$	h_i (W/m^2.k)	h_o (W/m^2.k)
1	1505.16	0.126	342.2	428.14
2	1896.55	0.147	372.8	587.59
3	2280.19	0.157	399.19	620.39
4	2665.34	0.167	423.18	660.13
5	3052.22	0.173	444.84	668.15

Table 11 includes the calculated values obtained as the hot water flow rate increases gradually.

Table 11 Tabulated data presenting calculated values for Case 2 (8 LPM)

Data No.	Q_h (W)	Q_c (W)	LMTD (^OC)	U (W/m^2.k)
1	1765.63	1223.07	27.85	183.53
2	1955.92	1393.33	27.97	212.06
3	2099.88	1449.07	28.13	219.23
4	2209.47	1504.8	28.34	234.72
5	2305.53	1672	28.2	252.33

Table 12 includes the calculated values obtained as the hot water flow while the cold water flow rate is held constant at 8 LPM.

Table 12 Tabulated data presenting calculated values for Case 2 (8 LPM)

Data No.	Re	$\mathcal{E}$	h_i (W/m^2.k)	h_o (W/m^2.k)
1	1517.21	0.137	343.08	535.3
2	1892.84	0.126	372.69	633.45
3	2275.77	0.11	399.17	616.09
4	2665.45	0.098	423.09	675.76
5	3046.22	0.096	445.23	760.79

Table 13 includes the calculated values obtained as the hot water flow rate increases gradually.

Table 13 Tabulated data presenting calculated values for Case 3 (12 LPM)

Data No.	Q_h (W)	Q_c (W)	LMTD (^OC)	U (W/m^2.k)
1	1765.63	1254	27.78	188.48
2	1990.55	1421.2	28.00	215.85
3	2141.43	1504.8	28.07	227.99
4	2257.98	1588.4	28.18	239.71
5	2415.78	1672	28.18	252.27

Table 14 includes the calculated values obtained as the hot water flow while the cold water flow rate is held constant at 12 LPM.

Table 14 Tabulated data presenting calculated values for Case 3 (12 LPM)

Data No.	Re	Ɛ	h_i (W/m^2.k)	h_o (W/m^2.k)
1	1487.81	0.143	341.1	580.71
2	1863.44	0.130	371.11	675.16
3	2280.71	0.116	400.3	687.82
4	2660.68	0.105	423.85	716.93
5	3040.72	0.097	445.41	760.2

Table 15 includes the calculated values obtained as the hot water flow rate increases gradually.

Table 15 Tabulated data presenting calculated values for Case 4 (16 LPM)

Data No.	Q_h (W)	Q_c (W)	LMTD (^OC)	U (W/m^2.k)
1	1848.39	1339.27	28.06	199.2
2	2024.71	1449.07	28.34	217.37
3	2223.53	1560.53	28.56	232.3
4	2353.88	1672	28.57	248.78
5	2470.54	1894.93	28.48	282.87

Table 16 includes the calculated values obtained as the hot water flow while the cold water flow rate is held constant at 16 LPM.

Table 16 Tabulated data presenting calculated values for Case 4 (16 LPM)

Data No.	Re	Ɛ	hi (W/m^2.k)	ho (W/m^2.k)
1	1487.67	0.151	340.89	706.52
2	1885.47	0.132	372.48	685.01
3	2271.36	0.118	399.15	733.14
4	2655.16	0.109	423.14	808.04
5	3034.47	0.109	444.77	1134.35

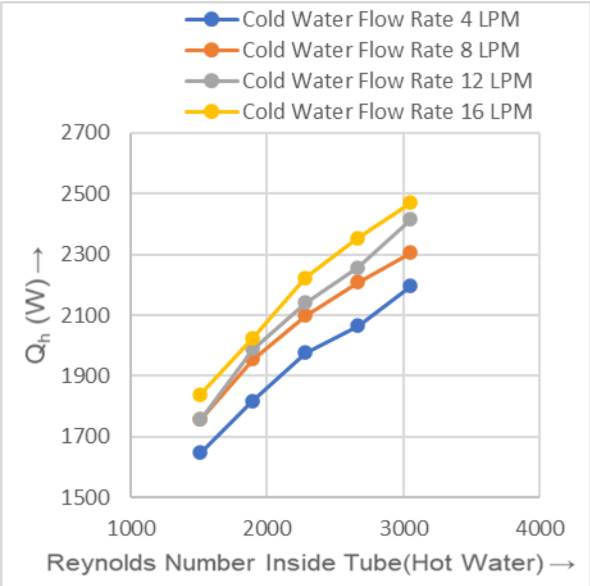

Fig. 10 Relation between hot water heat transfer rate and hot water Reynolds number

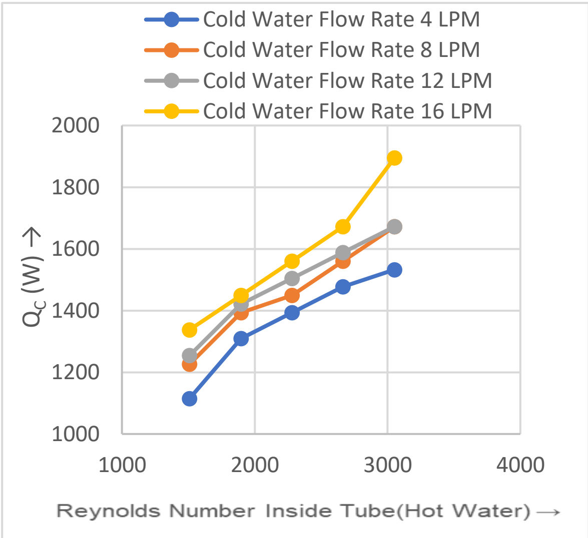

Fig. 11 Relation between cold water heat transfer rate and hot water Reynolds number

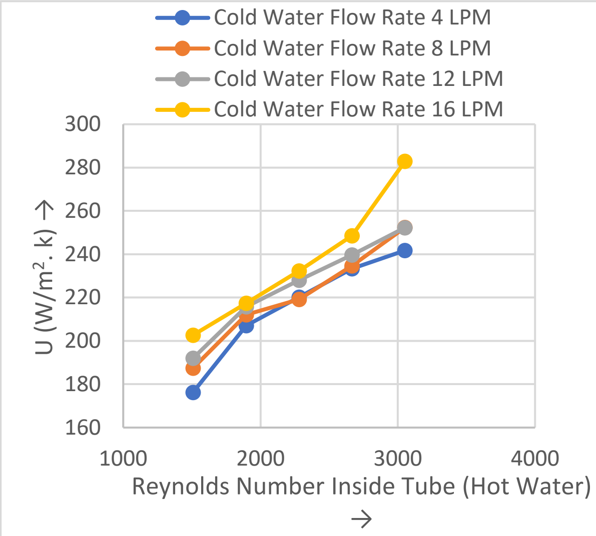

Fig. 12 Relation between LMTD and hot water Reynolds number

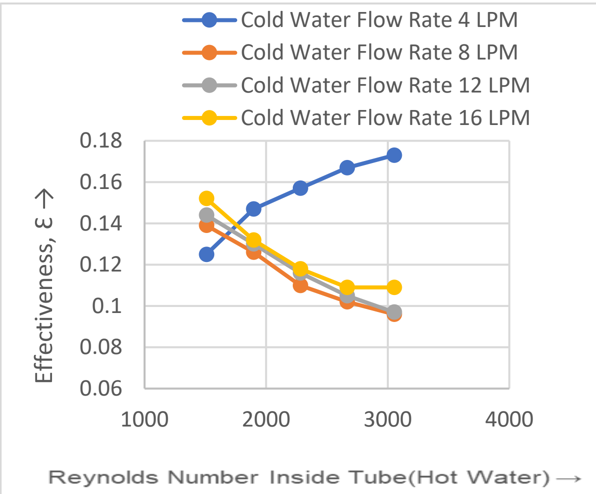

Fig. 13 Relation between overall heat transfer coefficient and hot water Reynolds number

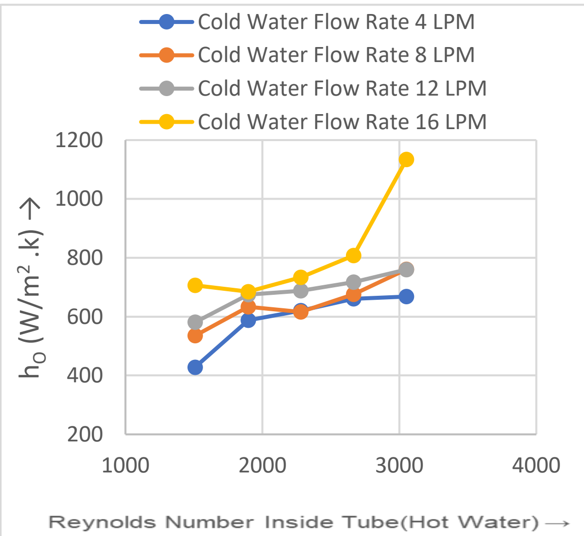

Fig. 14 Relation between effectiveness and hot water Reynolds number

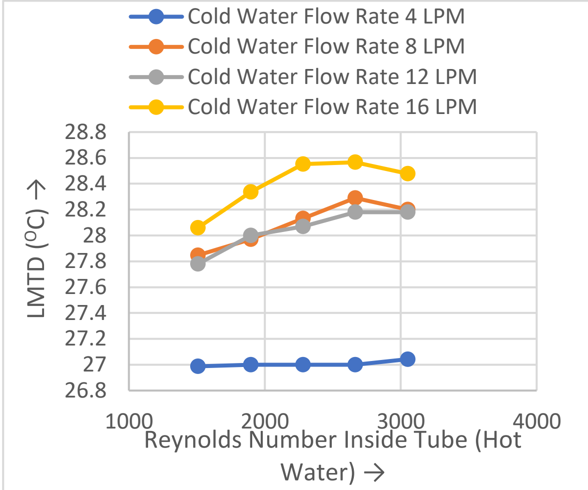

Fig. 15 Relation between convective heat transfer coefficient of the outside tube and hot water Reynolds number

5. Discussion

The conducted experiment on the shell and tube heat exchanger provided valuable insights, despite encountering some limitations and challenges. The variation in results can be attributed to the limitations of the setup. It was unfortunate that the mass flow rate could not be altered due to constraints in the water supply arrangements. This limitation prevented obtaining more comprehensive and accurate data to assess the performance of the constructed heat exchanger. The experiment had a number of assumptions. As tap water was used, heat losses across the outlet and inlet pipes were neglected. Additionally, the cold water temperature changed according to the surrounding temperature. Convection and radiation heat losses were also neglected. The size of the heat exchanger was smaller than the actual size. For this limited size, the limited amount of heat exchange and the temperature difference were achieved. In summary, the experiment provided valuable insights into the shell and tube heat exchanger's performance. It is also essential to acknowledge the limitations and challenges faced during the project. Future experiments should address these limitations by considering more accurate measurement techniques. These can be achieved by improving the heating mechanism and optimizing the design parameters.

6. Conclusion and Recommendations

In conclusion, the shell and tube heat exchanger project objectives were to construct the heat exchanger using appropriate materials and evaluate the heat transfer performance of the equipment. Several significant observations and findings were obtained by meticulous experimentation and data collection. The stainless steel is choice for heat exchanger materials for the long-term use. As an alternative, copper is a good material for making the tube. The heat transfer rates for the hot and cold water increase as the flow rate inside the tube for hot water increases, and the cold water flow rate at the outside is remained constant. If the constant cold water flow rates increase to the previous level, and the varying hot water flow rates remain the same as the previous rate. As a result, the heat transfer rate increases than previous rate.

The Log Mean Temperature Difference (LMTD) rapidly grows as the flow rate of hot water inside the tube increases. Parameters such as weight, size, and cost play essential roles in the design process, ensuring an optimal balance between performance and cost-effectiveness.
The construction of this device utilizes only ten tubes. Additional tubes can be incorporated into the apparatus to increase the heat transfer area, allowing for result comparison. Stainless steel is the chosen material for constructing this device. To achieve more satisfactory results, highly conductive materials such as copper or copper/nickel can be utilized. Furthermore, enhancing the heat transfer rate can be achieved by substituting water with nanofluids as the working fluid.

7. Acknowledgement

This work is financially supported by the Department of Mechanical Engineering, Chittagong University of Engineering and Technology, Chittagong-4349, Bangladesh, through the undergraduate research fund.

References

[1] Panta, M. and Panta, Y., 2025. Heat Exchanger Design and Optimization. Proceedings of the West Virginia Academy of Science, 97(2).

[2] Tancabel, J., Aute, V., Klein, E., Lee, C.Y., Hwang, Y., Ling, J., Muehlbauer, J. and Radermacher, R., 2022. Multi-scale and multi-physics analysis, design optimization, and experimental validation of heat exchangers utilizing high performance, non-round tubes. Applied Thermal Engineering, 216, p.118965.

[3] Tahery, A.A., Khalilarya, S. and Jafarmadar, S., 2017. Effectively designed shell-tube heat exchangers considering cost minimization and energy management. Heat Transfer—Asian Research, 46(8), pp.1488-1498.

[4] Tuncer, A.D., Sözen, A., Khanlari, A., Gürbüz, E.Y. and Variyenli, H.İ., 2021. Analysis of thermal performance of an improved shell and helically coiled heat exchanger. Applied Thermal Engineering, 184, p.116272.

[5] Shah, R.K. and Sekulic, D.P., 2003. Fundamentals of heat exchanger design. John Wiley & Sons.

[6] Sattar, E.A., Ouda, A.A. and Salman, M.D., 2023, July. Enhancement heat transfer in shell and tube heat exchanger by used hybrid and nanofluid. In 2ND INTERNATIONAL CONFERENCE ON ENGINEERING AND ADVANCED TECHNOLOGY:(ICEAT 2022) (Vol. 2787, No. 1, p. 030006). AIP Publishing LLC.

[7] Yılmaz, M.S., Ünverdi, M., Kücük, H., Akcakale, N. and Halıcı, F., 2022. Enhancement of heat transfer in shell and tube heat exchanger using mini-channels and nanofluids: an experimental study. International Journal of Thermal Sciences, 179, p.107664.

[8] Silaipillayarputhur, K., Al Mughanam, T., Al Mojil, A. and Al Dhmoush, M., 2017, December. Analytical and Numerical Design Analysis of Concentric Tube Heat Exchangers–A Review. In IOP Conference Series: Materials Science and Engineering (Vol. 272, No. 1, p. 012006). IOP Publishing.

[9] Tahery, A.A., Khalilarya, S. and Jafarmadar, S., 2017. Effectively designed shell-tube heat exchangers considering cost minimization and energy management. Heat Transfer—Asian Research, 46(8), pp.1488-1498.

[10] Hadad, K., Rahimian, A. and Rabiee, A., 2015. Nanofluid application in post SB-LOCA transient in VVER-1000 NPP. Annals of Nuclear Energy, 79, pp.101-110.

[11] Saffarian, M.R., Fazelpour, F. and Sham, M., 2019. Numerical study of shell and tube heat exchanger with different cross-section tubes and combined tubes. International Journal of Energy and Environmental Engineering, 10(1), pp.33-46.

[12] Wu, X.I.A.O., Kaifeng, W.A.N.G., Xiaobin, J.I.A.N.G. and Gaohong, H.E., 2016. Optimization of a shell-and-tube heat exchanger based on a genetic simulated annealing algorithm. Journal of Tsinghua University (Science and Technology), 56(7), pp.728-734.

[13] Ortega, R., Nikiforov, V. and Gerasimov, D., 2020. On modified parameter estimators for identification and adaptive control. A unified framework and some new schemes. Annual Reviews in Control, 50, pp.278-293.

[14] Ahmad, S., Linnhoff, B. and Smith, R., 1988. Design of multipass heat exchangers: an alternative approach.

[15] Monteiro Guimarães, L.G., dos Santos Guzella, M., Cabezas-Gómez, L. and Neves Teixeira, F., 2015. Numerical Determination of the LMTD Correction Factor for Shell-and-tube 1-2 Heat Exchangers. Applied Mechanics and Materials, 789, pp.457-461.

[16] Marzouk, S.A., Abou Al-Sood, M.M., El-Said, E.M., Younes, M.M. and El-Fakharany, M.K., 2023. A comprehensive review of methods of heat transfer enhancement in shell and tube heat exchangers. Journal of Thermal Analysis and Calorimetry, 148(15), pp.7539-7578.

[17] Qian, C., Wang, J., Zhong, H., Qiu, X., Yu, B., Shi, J. and Chen, J., 2024. Experimental investigation on heat transfer characteristics of copper heat exchangers based on triply periodic minimal surfaces (TPMS). International Communications in Heat and Mass Transfer, 152, p.107292.

[18] Hussien, A.A., Abdullah, M.Z. and Moh'd A, A.N., 2016. Single-phase heat transfer enhancement in micro/minichannels using nanofluids: theory and applications. Applied energy, 164, pp.733-755.

[19] Boujelbene, M., Mohammed, H.I., Sultan, H.S., Eisapour, M., Chen, Z., Mahdi, J.M., Cairns, A. and Talebizadehsardari, P., 2024. A comparative study of twisted and straight fins in enhancing the melting

and solidifying rates of PCM in horizontal double-tube heat exchangers. International Communications in Heat and Mass Transfer, 151, p.107224.

[20] Hariharan, K., Iams, A.D., Zuback, J.S., Palmer, T.A., Sridhar, N., Alazemi, R.M., Frankel, G.S. and Schindelholz, E.J., 2024. Enhanced localized corrosion resistance of Ni-based alloy 625 processed by directed energy deposition additive manufacturing. Corrosion Science, 230, p.111945.

[21] Dhavle, S.V., Kulkarni, A.J., Shastri, A. and Kale, I.R., 2018. Design and economic optimization of shell-and-tube heat exchanger using cohort intelligence algorithm. Neural Computing and Applications, 30(1), pp.111-125.

[22] SHAH, R.K., 1981. Research needs in low Reynolds number flow heat exchangers. Heat Transfer Engineering, 3(2), pp.49-61.